THE EFFECT OF SPLICE LENGTH AND DISTANCE BETWEEN LAPPED REINFORCING BARS IN CONCRETE BLOCK SPECIMENS

D. S. Sanchez[1] and L. R. Feldman[2]
[1] MSc Student, Department of Civil and Geological Engineering, University of Saskatchewan, Saskatoon, SK, S7N 5A9, Canada, denise.sanchez@usask.ca
[2] Associate Professor, Department of Civil and Geological Engineering, University of Saskatchewan, Saskatoon, SK, S7N 5A9, Canada, lisa.feldman@usask.ca

ABSTRACT
The mean lap splice resistance of No. 15 reinforcing bars with varying transverse spacing and lap splice length was evaluated in full-scale concrete block wall splice specimens. The range of the transverse spacing between bars was limited to that which allowed the bars to remain within the same cell, and included the evaluation of tied spliced bars in contact. A total of twenty-seven two-and-a-half blocks wide by thirteen course tall specimens reinforced with two lap splices were tested in four-point loading. All specimens were constructed in running bond with all cells fully grouted. The calculated mean tensile resistance of the reinforcement increased with increasing lap splice length, and was greater when the bars were in contact. Securing the bars in contact may have influenced the tensile capacity of the contact lap splices: higher stresses are likely to develop as a result of the bar ribs riding over each other with increasing slip. Results of the data analysis suggest that the tensile resistance of non-contact lap splices within the same cell is generally independent of the spacing between the bars; however, the slight decrease in the tensile resistance observed in select specimens with increased clear transverse spacing between the bars also suggests that the reduction in the cover distance to the block web influences bond capacity.

KEYWORDS: concrete block masonry, wall splice specimen, splice length, contact lap splice, non-contact lap splice

INTRODUCTION
Lap splicing is a common practice present in reinforced masonry construction. When a structure is taller or longer than the length of the typically produced reinforcing bars, lap splices provide the required continuity of the reinforcement. Frequently used at dowel locations or to accommodate obstructions such as openings or lintel beams, lap splicing is also a potential solution for reducing steel congestion. Lap spliced bars contained within a single block cell are usually not in direct contact as they are not typically tied together. A potential bond failure at the location of the splice may result if the resistance is less than in cases where continuous reinforcement is provided, and may be due to insufficient lap splice length or excessive transverse spacing between the spliced bars. Although previous research of non-contact lap splices in concrete specimens suggests that the spacing between spliced bars may actually enhance the bond performance of the reinforcement [1], a review of existing literature did not identify any similar studies related to masonry construction. Recent research performed by Ahmed and Feldman [2] included an evaluation of double pullout and wall splice concrete block

specimens reinforced with contact and non-contact lap splices, though the scope of the project was limited to non-contact splices in adjacent cells, 300 mm lap splice lengths, and 15 mm diameter reinforcing bars.

This paper presents the details and analysis results of an experimental investigation designed to evaluate the mean splice resistance given varying lap splice lengths and transverse bar spacings for No. 15 lapped reinforcing bars located within the same cell in full-scale concrete block wall splice specimens. Visual observations of the failure modes, crack propagation patterns, and internal damage for the different reinforcing configurations tested are also described and critically reviewed.

EXPERIMENTAL PROGRAM

Twenty-seven wall splice specimens were constructed and tested within this experimental program. Table 1 shows the nine different combinations of splice length and lateral bar spacing values selected based upon the results of previous research, which had demonstrated that a 300 mm lap splice length is capable of developing the nominal yield capacity of Grade 400, No. 15 reinforcing bars [2]. Three shorter lap splice lengths were selected in an attempt to ensure bond failure of the wall splice specimens in combination with the three transverse spacings used for each. Each such configuration ensures proper encapsulation of the spliced bars based on typical construction practices and accounts for the CSA Standard A371-04 [3] provisions for the minimum continuous unobstructed cell space of 50 mm x 74mm that must be provided in all masonry structures. Three replicate specimens were constructed for each reinforcement configuration in order to validate the results. Table 1 also shows that the construction and testing of the total number of walls was carried out in two phases. Details of the test specimens, material properties, and experimental setup are provided as follows.

Table 1: Reinforcement Configurations Tested in the Wall Splice Specimens

Splice length (mm)	Lateral bar clear spacing (mm)
150	0[2], 25[1], 50[2]
200	0[2], 25[1], 50[2]
250	0[2], 25[2], 50[2]

[1] *Tested as part of the first phase of the experimental program.*
[2] *Tested as part of the second phase of the experimental program.*

Figure 1 shows the overall dimensions of the wall splice specimens. Wall splice specimens were two-and-a-half blocks wide and thirteen courses tall and were constructed in a running bond pattern with all cells fully grouted. Figure 1(a) shows the elevation of the wall splice specimens. All specimens were reinforced with No. 15 bars in the cells as shown with the splices provided at mid-height. Figure 1(b) shows a cross-section of the specimen within the mid-height splice region and shows that a template made of commercial welded wire mesh was placed in the bed joints immediately above and below the seventh block course to maintain the proper alignment of the reinforcement. The spliced reinforcing bars were centered within the common grouting cell space and extended approximately 190 mm above and below the top and bottom of the wall specimens, respectively.

All wall splice specimens were constructed by a journeyman mason in two lifts. A first lift of 8 courses was constructed and grouted to provide full embedment of the bottom reinforcement and all reinforcement within the lap splice length. The grout was allowed to set for a minimum of 12 hours before the construction of the 5 course second lift. After construction, all specimens were cured for a minimum of 28 days in the laboratory environment prior to testing.

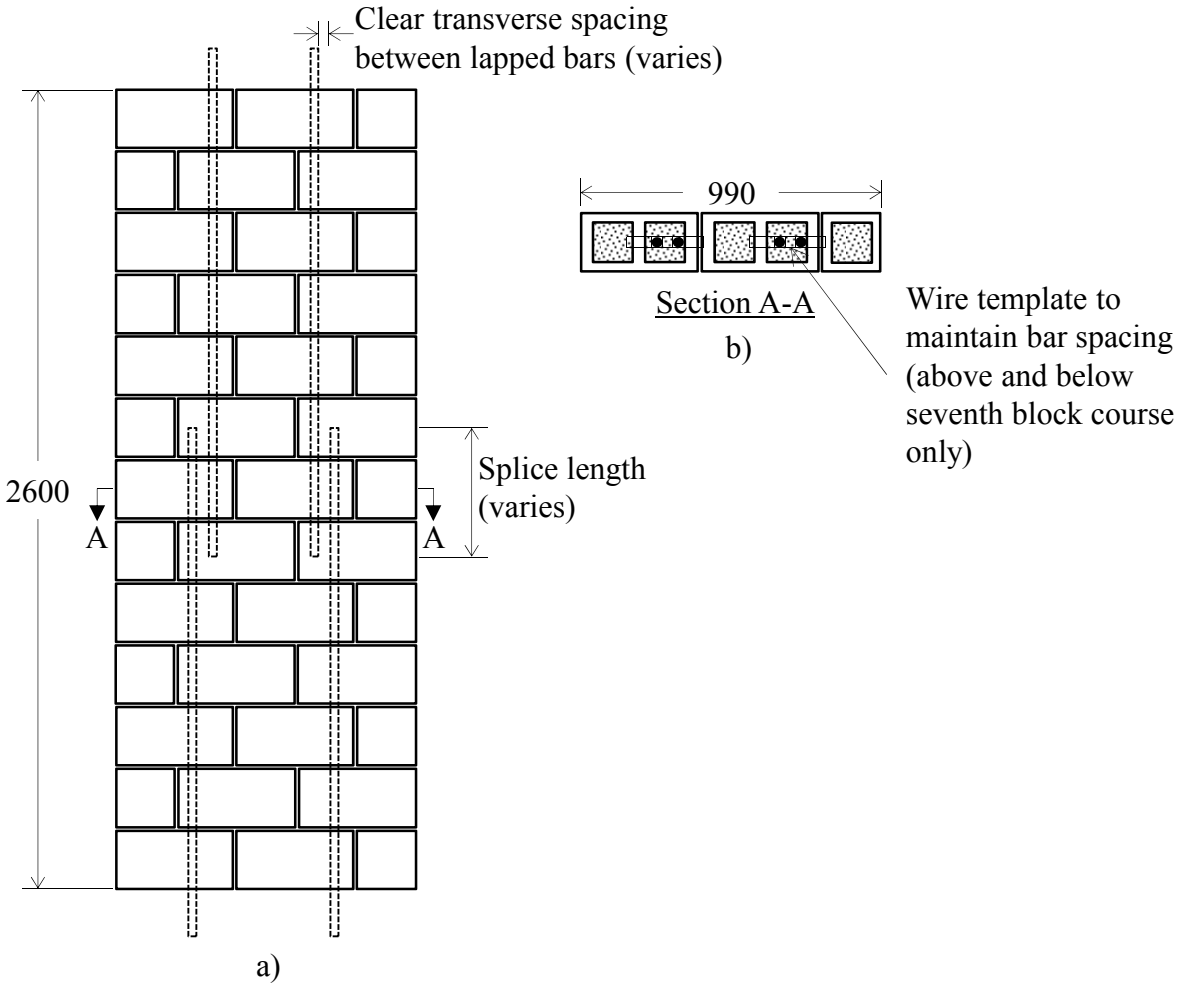

Figure 1: Wall Splice Specimen Geometry: a) Elevation; b) Cross-Section Within the Lap Splice Length

Table 2 summarizes the material properties as obtained from the companion specimens tested along with each of the wall splice specimens. All companion specimens were stored and cured under the same laboratory environmental conditions as the wall splice specimens.

Standard flat and frogged ended hollow concrete masonry blocks (390 mm long x 190 mm wide x 190 mm tall), meeting the specifications provided in CSA Standard A165-04 [4], were used. Half blocks were cut in the laboratory using a masonry brick/block saw rather than ordering half blocks in order to ensure all blocks within each specimen had the same material properties. The mean compressive strength of the masonry units was calculated based on the resulting load test

data and the average net cross-sectional area of the blocks as obtained from an absorption test conducted in accordance with ASTM C140-10 [5].

Table 2: Summary of the Mean Material Properties of the Companion Specimens Tested Along With the Wall Splice Specimens

Type of companion specimen	Phase no.	No. of specimens tested	Mean compressive strength (MPa)	COV* (%)
Masonry block	I	8	25.4	6.42
	II	10	23.4	8.13
Mortar cubes	I	6	18.9	12.8
	II	21	13.5	11.5
Grout cylinders	I	12	18.7	10.8
	II	20**	14.1	8.26
Absorptive grout cylinders	I	12	18.4	12.3
	II	21	16.2	11.0
Masonry prisms	I	5**	12.7	2.83
	II	21	12.5	12.5

**COV: Coefficient of variation*
***One outlier was identified that is not included in the results presented in this table*

Laboratory prepared Type S mortar with a minimum 28-day nominal compressive strength of 12.5 MPa, and a 1:3 mortar cement to sand proportion by volume, prepared in accordance with CSA Standard A179-04 [6], was used throughout. The fine aggregate used in the mortar mix was graded in accordance with CSA Test Method A23.2-2A [7], and complied with the standard requirements of CSA A179-04 [6]. Mortar cubes were prepared and subsequently tested in accordance to CSA Standard A3004-C2 [8] at a constant rate of 10 kN/min.

High slump grout with a high water/cement ratio, in accordance with CSA Standard A179-04 [6], was mixed in the laboratory and hand placed in the cells of the wall splice specimens. A measured slump of about 250 mm and a minimum 28-day compressive strength of 12.5 MPa resulted. Type GU Portland cement and pre-mixed gravel with a maximum aggregate size of 10 mm, in accordance with CSA A179-04 [6], were provided by a local supplier for grout preparation. Material properties for the grout were established from the non-absorptive cylinders and absorptive specimens tested along with the wall specimens. Non-absorptive cylinders (100 mm diameter x 200 mm high) were cast and tested in accordance with CSA A179-04 [6], and absorptive specimens (100 mm wide x 100 mm long x 190 mm high) were cast and tested in accordance with ASTM C1019 [10].

Three block high by one block wide masonry prisms were constructed and tested on the same day as each wall splice specimen to establish the mechanical properties of the masonry assemblage. Masonry prisms were tested in accordance with CSA Standard S304-04 Annex D [11] at constant loading rate of a 1 kN/s. Two linear variable differential transducers (LVDTs) were attached to the face shell at the mid-height of the top and bottom blocks to measure the vertical deformation of the specimens as testing progressed.

Grade 400 hot-rolled deformed reinforcement with a nominal diameter of 15 mm was used in all specimens. A total of 6 samples were obtained from each of the two heat batches used during construction, and were tested in accordance with ASTM Standard A370-11 [9] to establish the actual material properties for the two construction phases. The reinforcing bar samples corresponding to the first construction phase had a yield stress, f_y, equal to 434 MPa, a modulus of elasticity, E_s, of 174 GPa, a strain at the initiation of strain hardening, ε_{sh}, equal to 0.014, and an ultimate stress, f_{ult}, of 611 MPa. Samples tested in conjunction with the second construction phase had a yield stress, f_y, of 434 MPa, a modulus of elasticity, E_s, equal to 180 GPa, a strain at the initiation of strain hardening, ε_{sh}, of 0.013, and an ultimate stress, f_{ult}, equal to 615 MPa.

A steel frame consisting of two horizontal beams connected by threaded bars was assembled as a rigging frame to safely secure the walls while transporting and rotating them to the testing position using an overhead crane. End anchorages were provided at the wall ends prior to testing to prevent bar slippage and ensure failure would occur within the lap splice region. The anchorages consisted of 200 mm square x 8 mm thick steel plates, with a drilled hole in their centre, and were secured against the specimen ends by means of mechanical reinforcing bar couplers tightened onto the excess bar lengths that extended beyond both ends of the wall splice specimens. A layer of mortar was used as a levelling compound to ensure full contact between the specimen and the steel plates.

Figure 2 shows the four-point loading setup and instrumentation used in the testing of the wall splice specimens. Six LVDTs were used to measure the vertical displacement at different locations along the specimen length. Two LVDTs were located on each side of the wall at the specimen centreline, while the remaining four LVDTs, were located at 200 and 600 mm on either side of the specimen centerline (i.e. one specimen side only was instrumented at the four locations). The load was applied by an MTS hydraulic actuator at the centerline of a spreader beam. The contact points between the spreader beam and the wall splice specimen were such that the four-point loading arrangement shown in Figure 2 was achieved. Load was applied at a constant displacement of 0.5 mm/min until failure, defined as a 60% load reduction from that recorded at the maximum carrying capacity.

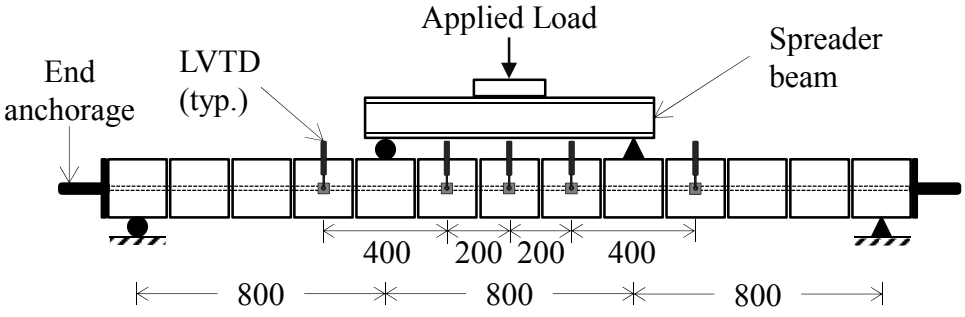

Figure 2: Wall Splice Specimen Test Setup and Instrumentation Details (Modified From Ahmed and Feldman [2])

RESULTS OF WALL SPLICE SPECIMEN TESTS

Table 3 presents the mean ultimate failure load and calculated average tensile resistance for the different splice configurations as calculated based on tests of the three replicate specimens for

each. The notation system used to identify each set of wall replicates consists of two parts separated by a forward slash. The first number indicates the splice length in millimetres preceded by the letter 'W' for wall splice specimen. The second number (i.e. following the forward slash) corresponds to the clear transverse spacing between the lapped bars in millimetres. The mean values of cracking and ultimate failure loads were directly obtained from the test results by averaging the recorded data as obtained from the MTS actuator load cell for each specimen. A numerical analysis, based upon the ultimate recorded load and the stress versus strain relationship for the companion specimens, was performed to obtain the maximum splice tensile resistance of the wall splice specimens and is discussed in detail later in this section.

Table 3: Summary of Load History and Splice Capacity for the Different Splice Configurations Tested in the Wall Splice Specimens

Splice configuration	Mean values of:				
	Measured cracking load (kN)	Midspan deflection at ultimate load (mm)	Ultimate failure load (kN)	Theoretical curvature at ultimate moment (1/m)	Tensile resistance of the reinforcement (kN)
W150/0	5.43	12.0	21.2	0.0317	74.3
W150/25	4.27	10.7	19.4	0.0303	69.5
W150/50	4.67	9.06	19.5	0.0300	70.5
W200/0	5.60	15.2	33.0	0.331	97.2
W200/25	4.93	11.6	22.6	0.0343	78.4
W200/50	6.15	11.8	21.2	0.0327	74.5
W250/0	3.96	17.5	35.1	0.334	97.7
W250/25	6.60	12.9	26.3	0.129	84.2
W250/50	6.44	11.7	25.1	0.0850	82.1

Figures 3, 4 and 5 show the load versus midspan deflection curves for representative specimens with 150 mm, 200 mm and 250 mm lap splice lengths, respectively. Each figure shows the results for all three values of clear transverse spacing as tested. In general, the load-deflection response for all of the reinforcement configurations can be divided in two stages prior to the attainment of the maximum load. In the first stage, a linear increase from the origin to the load that represents first cracking for the specimens is noted. In the second stage, the applied load continued to increase linearly with increasing deflection at a reduced slope until failure. Some visible sudden decreases in the load (i.e. noise) were associated with the formation of additional cracks. A slight reduction in slope before the ultimate load, most likely caused by a reduction in stiffness due to bond loss at the location of the splice [2], as well as a brief gradual unloading curve after peak load, suggests brittle failure occurred for all splice configurations. Inelastic behaviour, indicating yielding of the reinforcement, was only observed in one of the W250/0 replicates starting at an applied load of 36 kN; and roughly coincided with the theoretical yielding load of the reinforcement. Each of Figures 3 to 5 shows that the experimental load versus midspan deflection curves for the different reinforcement arrangements generally agreed well with the theoretical curves derived for each splice length configuration.

The load versus midspan deflection curves for all specimens with a 150 mm splice length had similar load-midspan deflection behaviour regardless of the clear transverse spacing provided

between the lap spliced bars. In contrast, specimens reinforced with 200 and 250 mm lap splices in contact generally attained about 29% and 35% higher midspan deflections respectively, as compared to those in which a non-zero clear transverse spacing was provided. In general, contact lap splices caused a slight increase in the flexural strength of the wall specimens; however, no definite pattern could be clearly identified for the specimens with non-contact lap splices.

The observed crack patterns were similar for all specimens. Flexural cracks were only observed in the mortar joints and typically propagated from the joints adjacent to the points of applied load to the joints adjacent to the specimen centreline and up to the third or fourth joints adjacent to the supports. The widest cracks, usually those that caused specimen failure, were typically the cracks that developed in the joints adjacent to the centre course. Figure 6 shows the open flexural crack identified as the common failure mode for the wall splice specimens for all reinforcement configurations.

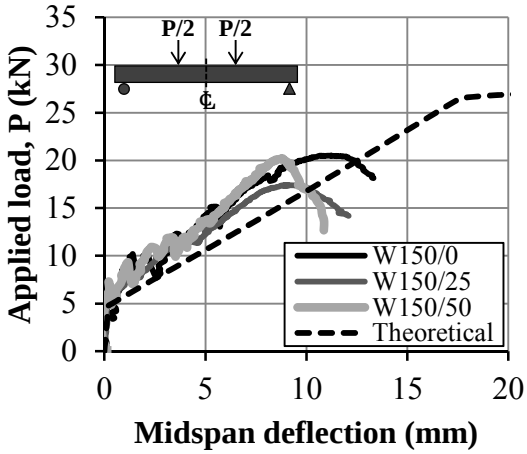

Figure 3: Representative Load Versus Midspan Deflection Curves for Specimens with a 150 mm Lap Splice Length

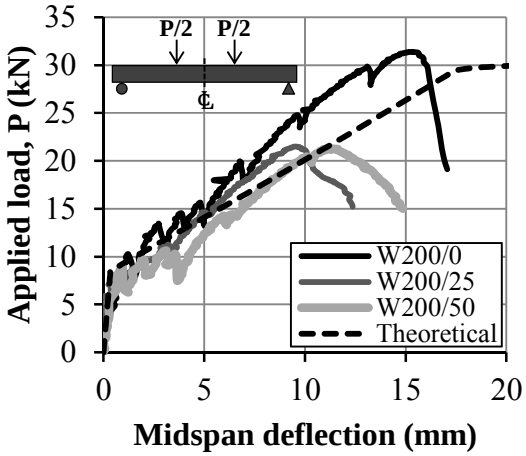

Figure 4: Representative Load Versus Midspan Deflection Curves for Specimens with a 200 mm Lap Splice Length

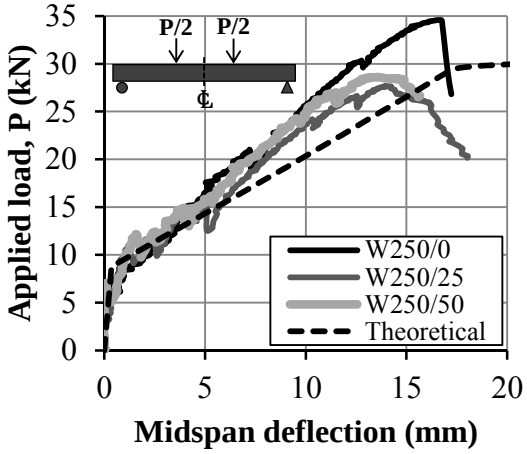

Figure 5: Representative Load Versus Midspan Deflection Curves for Specimens with a 250 mm Lap Splice Length

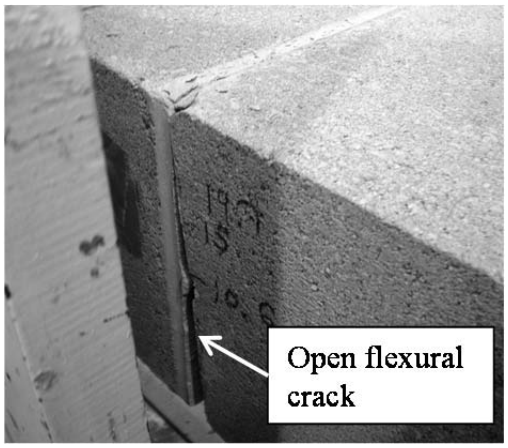

Figure 6: Typically Observed Failure Mode for the Wall Splice Specimens

The face shell and grout surrounding the reinforcement were removed following testing for select random specimens for each splice configuration to investigate internal cracking patterns and bond deterioration within the lap splice length. Figure 7 shows the typical internal damage as observed in the specimens reinforced with contact lap splices (i.e. W150/0, W200/0, and W250/0 arrangements). Crushing of the grout between the reinforcing bar lugs and consequent bar pullout were observed, indicating that a bond failure between the reinforcement and the grout occurred in these specimens. Splitting cracks extending between the spliced bars through the grout and along the block-grout interface toward the mortar joints were identified, suggesting poor bond between the grout and the concrete blocks. The voids existing between block ends, areas of poor grout consolidation, also facilitated the crack propagation along the mortar joints [2].

Figure 8 shows the characteristic internal damage and crack propagation observed in specimens reinforced with non-contact lap splices with a 25 mm clear transverse spacing between the spliced bars (i.e. W150/25, W200/25, and W250/25 configurations). Similar to specimens with contact lap splices, crushing of the grout keys between lugs as well as bar pullout were observed in specimens with 200 and 250 mm lap splice lengths. Inclined struts between the lapped bars, in addition to cracks extending vertically from the bar ends through the grout and to the mortar joints, were identified. Bar pullout and cracking between the spliced bars were less evident for specimens with a 150 mm lap splice length, though crack propagation from the bar ends to the mortar joints occurred as in the specimens with longer lap splice lengths. Cracks in specimens with a 50 mm clear transverse spacing between the lap spliced bars (i.e. W150/50, W200/50, and W250/50 configurations), generally extended from the reinforcing bars to the closest grout-block interface and to the mortar joints. Crushing of the grout between lugs, bar pullout, and cracks in the remaining grout between lapped bars were less evident as compared to specimens with lesser values of clear transverse spacing between the lap spliced bars.

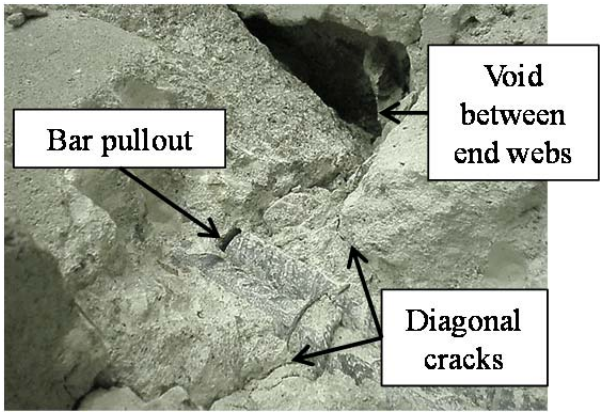

Figure 7: Internal damage and crack propagation observed in specimens with contact lap splices

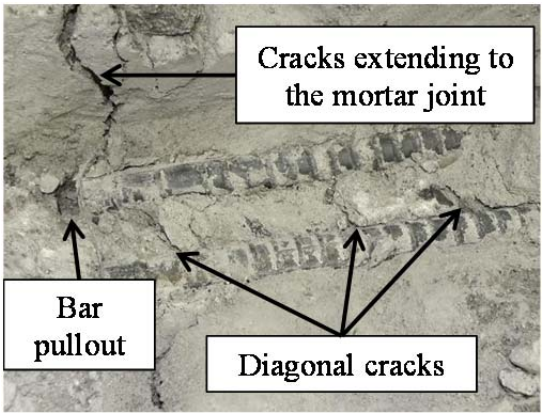

Figure 8: Internal damage and crack propagation observed in specimens with 25 mm splice-bar spacing

A numerical finite difference analysis was performed to calculate the maximum tensile resistance of the spliced reinforcing bars in the wall splice specimens based upon the moment-curvature response derived for the specimens as internal strain gauges were not used to instrument the reinforcing bars. The analysis, similar to that adopted by Ahmed and Feldman [2], was based

upon the mechanical properties of the masonry assemblage and the reinforcing steel as obtained from the companion specimens tests, and the load history of the wall splice specimens. The theoretical stress versus strain relationship for the masonry assemblage was first derived by fitting the experimental data obtained for the companion masonry prisms to a modified Park-Kent curve [12]. The average mechanical properties of the reinforcing bar samples from each heat batch were also used to derive the theoretical tensile stress-strain profile for the steel, assuming a parabolic curve for the strain hardening region. The theoretical stress-strain curves derived for the masonry assemblage and the reinforcing steel agreed well with the experimental stress-strain curves obtained from the companion specimen tests.

The theoretical moment-curvature relationships for the wall splice specimens were calculated based upon the internal moment effect resulting from the applied load level throughout testing. The curvature of the uncracked masonry section (ϕ_{uc}) was obtained directly from the ratio of the internal moment at mid-height divided by the flexural rigidity of the gross section (M/EI_{gr}). An iterative procedure, which divided the compression zone into 100 layers of equal depth, was then used to establish the neutral axis depth (c) of the cracked section at a given moment (M), based on the equilibrium of the compressive strength of the masonry assemblage and the tensile force in the reinforcement ($C=T$). The tensile resistance (T) in the reinforcement was finally computed from the theoretically calculated curvature at the ultimate moment, as the product of the tensile stress in the reinforcement at the corresponding strain multiplied by the nominal cross-sectional area of the reinforcing bars (A_s). A theoretical moment-curvature curve was developed for each splice length and transverse spacing between the lap spliced bars. In general, good agreement was obtained between the experimental and theoretically calculated deflected profiles for the wall splice specimens.

Figure 9 shows a summary of the calculated mean splice tensile resistance as obtained for each set of replicate wall splice specimens. The error bars shown for each reinforcement configuration show the range of individual test results as calculated for the replicate specimens. The calculated range of results obtained for specimens with contact lap splices with a 250 mm splice length (i.e. W250/0) was small and so is not evident in Figure 9. In general, results show that the tensile capacity of the contact lap splices was higher as compared to that calculated for the non-contact lap splices with the same splice length. This increased tensile capacity, however, was more evident for the two longer lap splice lengths. The fact that the lapped reinforcing bars in contact were tied with wire at both ends of the splice may also have enhanced the splice capacity of the reinforcement, as higher stresses are likely to develop between the ribs of the bars as they ride over each other with increased slip. Such practice is not common within the masonry industry.

Non-contact lap splices behaved similarly regardless of the lateral bar spacing provided. However, a slight decrease in tensile capacity with increasing transverse spacing was noted for specimens with 200 mm and 250 mm lap splice lengths. The cover distance to the adjacent block web, which is less than the cover distance to the block flanges when the bars are not in contact, may have influenced the bond capacity. The poor bond between the grout and the blocks, and the low strength of the mortar joints associated with masonry, proved to have direct effect in the bond capacity and led to a failure of the splice in all reinforcement configurations.

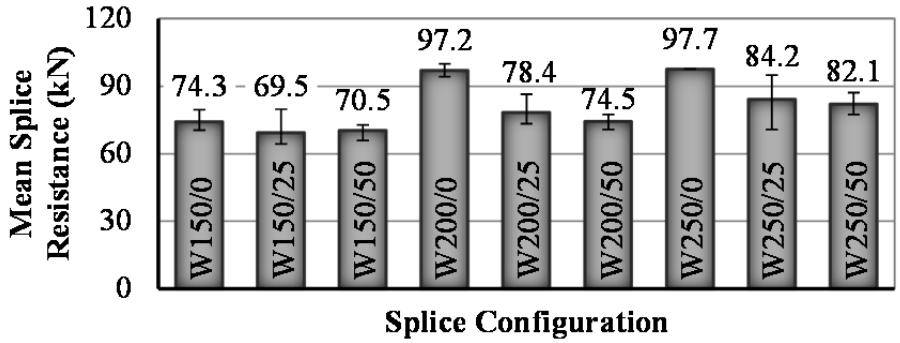

Figure 9: Summary of the Calculated Mean Splice Tensile Resistance for Each Set of Wall Splice Specimens

SUMMARY AND CONCLUSIONS

This paper presents the results of an experimental program consisting of 27 wall splice specimens reinforced with No. 15 lap spliced reinforcing bars tested in four-point loading. Three lap splice lengths (150 mm, 200 mm, and 250 mm) and three different values of lateral bar spacing (0 mm, 25 mm, and 50 mm), such that the lap spliced bars were each contained within a single block cell, were tested. Three replicate specimens were tested for each reinforcing bar geometry. All specimens were 2-1/2 blocks wide and thirteen courses tall, and were constructed in running bond with all cells fully grouted.

The following conclusions and observations were noted:

1. A wide flexural crack on the tension face, typically located in the bed joints adjacent to the central block course, was identified as the common cause of failure for all of the wall splice specimens. Flexural cracks were only observed in the mortar joints and typically occurred within the midspan region up to the third or fourth last joint adjacent to each support. Lap splice failure due to a loss of bond between the reinforcement and the surrounding grout was observed in all specimens.
2. The mean tensile resistance of the lap spliced reinforcing bars in contact, regardless of the splice length, was higher than that calculated for the non-contact lap splices with the same splice length. The use of tie wire to ensure contact between the lapped bars is not a typical practice used in construction and likely caused an increased capacity as a result of the higher stresses developed due to the bar ribs riding over each other with increased slip.
3. Non-contact lap splices behaved similarly regardless of the lateral bar spacing provided though a slight decrease in the mean tensile capacity of the lapped bars with 50 mm transverse spacing as compared to the 25 mm-spaced bars was observed, particularly for specimens with 200 and 250 mm lap splice lengths. The reduction in the clear distance between the bars and the webs of the block as the transverse spacing between bars increased likely affected bond performance.
4. The poor bond between the grout and the blocks, and the low strength of the mortar joints associated with masonry proved to have direct effect on the bond capacity.

ACKNOWLEDGEMENTS

The authors would like to thank Brennan Pokoyow ay and Dale Pavier, Structures Laboratory Technicians, and journeym an masons Kim Parenteau and Roy Nicolas from Gracom, for their assistance with the execution of the experim ental program. Financial support was provided by the Saskatchewan Mas onry Institute (SMI), the Saskatch ewan Centre for Maso nry Design (SCMD), the Natural Sciences and Engineering Research Council of Canada (NSERC), and the University of Saskatchewan.

REFERENCES

1. Hamad, B.S. and Mansour, M. (1996) "B ond Strength of Non-C ontact Tension Lap Splices", ACI Structural Journal, V. 93, No. 3, p. 316 – 326.
2. Ahmed, K. and Feldm an, L.R. (2012) "Evalu ation of Contact and N on-Contact Lap Splices in Concrete Block Masonry Cons truction", Canadian Journal of Civil Engineering, V. 39, No. 5, p. 515 – 525.
3. CSA (2004) "CAN/CSA A371-04 (R2009) Masonry Construction for Buildings", Canadian Standards Association, Rexdale, ON, Canada.
4. CSA (2004) "CAN/CSA A165 Series-04 (R2009) CSA Standards on Concrete Masonry Units", Canadian Standards Association, Rexdale, ON, Canada.
5. ASTM (2010) "ASTM C140-10 Standard T est Methods for Sa mpling and Testing Concrete Masonry Units and Related Units", ASTM International, W est Conshohocken, PA, USA.
6. CSA (2004) "CAN/CSA A179-04 (R2009) Mort ar and Grout fo r Unit Masonry", Canadian Standards Association, Rexdale, ON, Canada.
7. CSA (2009) "CAN/CSA A23.2-2A-09 Concrete Materials and Meth ods of Concrete Construction/Test Methods and Standard Prac tices for Concrete", Canadian Stand ards Association, Rexdale, ON, Canada.
8. CSA (2008) "CAN/CSA A3000-08 Ce mentitious Materials Compendium", Canadian Standards Association, Rexdale, ON, Canada.
9. ASTM (2011) "ASTM A370-11 Standard Test Methods and Definitions for Mechanical Testing of Steel Products", ASTM International, West Conshohocken, PA, USA.
10. ASTM (2011) "ASTM C1019-11 Standard T est Method for Sa mpling and Testing Grout", ASTM International, West Conshohocken, PA, USA.
11. CSA (2004) "CAN/CSA S304.1-04 (R2010) Design of Masonry Structures", Canadian Standards Association, Mississauga, ON, Canada.
12. Park, R., Pries tley, M.J.N., and Gill, W .D. (1982) "Ductility of Square Confined Concrete Columns", Journal of the Structural Division, V. 108, No. 4, p. 929-950.